www.dergipark.gov.tr
ISSN:2148-3736
El-Cezerî Fen ve Mühendislik Dergisi
Cilt: 7, No: 2, 2020 (940-969)

El-Cezerî Journal of Science and Engineering
Vol: 7, No: 2, 2020 (940-969)

ECJSE

DOI :10.31202/ecjse.672615

**Makale/Research Paper**

# Past and Present Approaches to Borosilicate Glasses

**Bekir KARASU, İrem DEMİREL, Soykan AYDIN, Metehan DALKIRAN, Beyza LİK**

Eskişehir Technical University, Department of Materials Science and Engineering, Eskişehir/ Türkiye
bkarasu@eskisehir.edu.tr

**Received/Geliş:** 09.01.2020 **Accepted/Kabul:** 10.03.2020

**Abstract:** Thanks to their distinguished properties borosilicate glasses (BSGs) are preferred in many application fields: laboratory glassware, microwave glass cookware, high–quality beverage glassware, aquarium heaters, flashlights, spotlights (high–powered lighting products), high-intensity discharge lamps, telescopes, biomaterials, immobilization and disposal of radioactive wastes, microscope lenses and slides, art construction, aviation (airplanes, UAVs, missiles), etc. This work aims to present general information about BSGs.

**Keywords:** Borosilicate glass; history; development; properties; application

# Borosilikat Camlarına Yönelik Geçmişte ve Günümüzdeki Yaklaşımlar

**Öz:** Sahip oldukları seçkin özellikleri sayesinde borosilikat camlar pek çok uygulamada kendilerine yer bulmaktadırlar: laboratuvar gereçleri, mikro dalga cam ürünleri, yüksek kalitede sofra ürünleri, akvaryum ısıtıcıları, spot aydınlatmaları, teleskoplar, biyo uygulamalar, radio aktif atıkların güvenli bir biçimde uzaklaştırılması, sanatsal yapılar, havacılık uygulamaları (uçaklar, füzeler) vb. Bu derleme makalesinin amacı borasilikat camları hakkında genel bilgi sunmaktır.

**Anahtar Kelimeler:** Borosilikat cam; tarihçe; gelişim; özellikler; uygulama

## 1. Introduction

Borosilicate glass (BSG) is a special sort of glass consisting of $SiO_2$ and $B_2O_3$ and commonly employed thanks to its worthwhile features. It generally has a lower thermal expansion coefficient value ($3.4 \times 10^{-6}$ °$C^{-1}$) than that of soda–lime–silica (SLS) glass, and possesses good chemical resistance, high dielectric strength and a higher softening temperature (800 °C) when compared to those of SLS glass. It is also less dense than the usual soda–lime glass with a comparingly low refractive index (Fig. 1). Therefore, it is employed for the manufacturing of laboratory glassware (Fig. 2), household cookware, industrial piping, bulbs for hot lamps and electronic tubes of high wattage such as x–ray tubes. Furthermore, BSG is very important in the production of Vycor glass, containing about 96 % $SiO_2$ and is a crucial substitution for fused silica (FS). Vycor glass could be manufactured

*How to cite this article*
Karasu, B., Demirel, İ., Aydın S., Dalkıran M., Lik B., "*Past and Present Approaches to Borosilicate Glasses*", El-Cezerî Journal of Science and Engineering, 2020, 7 (2); 940-969.

*Bu makaleye atıf yapmak için*
Karasu, B., Demirel, İ., Aydın S., Dalkıran M., Lik B., "*Borosilikat Camlarına Yönelik Geçmişte ve Günümüzdeki Yaklaşımlar*", El-Cezerî Fen ve Mühendislik Dergisi 2020, 7 (2); 940-969.

at lower working temperatures when compared to FS, being of economic interest. It is employed, for example, in projection lamps [1].

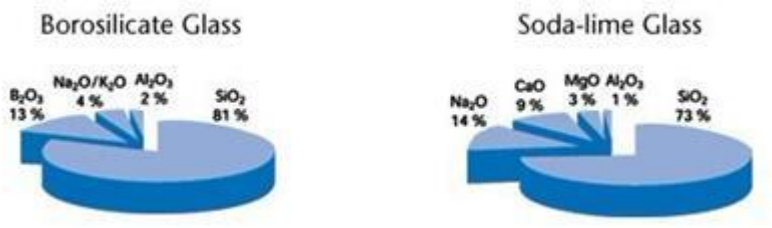


Figure 1. Chemical compositions of borosilicate and soda–lime glasses [2]

Besides being technologically important, the precise glass–forming zones and phase relationships in BSGs were not sorted out yet. Additionally, the knowledge of the molecular groups in them is scattered and not completed [1].

Figure 2. Some BSG wares for laboratories [3]

## 2. History

Humans have been producing glass for approximately 5,000 years, making BSG one of the oldest manufactured materials in the World. The Babylonians were known as the nation imported borax from the Far East over 4000 years ago as a fluxing agent to work gold. There is rigid evidence that tincal ($Na_2B_4O_7.10H_2O$) was firstly employed in the 8$^{th}$ century around Mecca and Medina. Türkiye's borate industry commenced in 1865 with mining pandermite ($4CaO_5.B_2O_3.7H_2O$). Approx. at the same time, various deposits of borate have been found in California and Nevada, including ulexite ($Na_2O_2.CaO.5B_2O_3.16H_2O$) and colemanite ($2CaO.3B_2O_3.5H_2O$) in Death Valley. As a result of a reaction with trona ($Na_2CO_3.NaHCO_3.2H_2O$), they could be converted to borax. The Kramer deposit in California was found in 1913, first as colemanite. In 1926 tincal was discovered, rasorite (kernite, $Na_2O.2B_2O_3.4H_2O$) was met. Türkiye offered colemanite for many years to European boric acid manufacturers [4].

The invention of BSG is usually attributed to Otto Schott, a German glassmaker and was commercialized with the name of "Duran" in Europe in 1893 [5]. In summer 1893 the Glastechnisches Laboratorium put borosilicate laboratory glassware on the market for the first time. The 100$^{th}$ anniversary of Schott laboratory glass should be the occasion to present the pioneer BSG research by Otto Schott. At first, he developed glass containing boric acid for optics with improved and predictable optical properties. Based on this work, he turned to technical glass. Thermometer glass, laboratory glass, and lamp chimneys were the first fields of application for chemically and thermally resistant BSG. Otto Schott's invention paved the way for glass as a material to advance into new dimensions and provided the basis for important scientific and technical progress. With the development and mass production of ready–to–use BSG, the Glastechnisches Laboratorium rose from a scientifically based handwork to a leading international group in the special glass sector. Schott still sells it under this name today. In the US, BSG was first produced by Corning Glass Works in 1915 and sold with the name of Pyrex.

During the 1880s, Abbe and Schott, for the first time, used boron compounds in glass in significant amounts. Faraday and Harcourt had also employed boron in glass, but Abbe and Schott established that BSGs possessed outstanding endurance to chemical attack when compared to soda–lime–silica (SLS) glasses and better thermal shock resistance thanks to their lower thermal expansion coefficient. In 1887 Auer von Welsbach introduced mantle in gas lamps. Schott met this requirement with a glass having 15 % $B_2O_3$. At this time in the US, cracking and breakage of the globes of railroad brakemen's lanterns was a problem when rain showers struck the hot glass. In 1908 Corning Glass Works, US leading lamp chimneys and bulbs manufacturer became the first newly formed research laboratory investigating this matter. In 1909, Corning introduced a BSG for solving the mentioned problem but the glass had poor chemical endurance. Eugene C. Sullivan from Corning and William C. Taylor collaborated on this issue. By 1912, they made a highly chemically durable, shock–resistant, Pb–BSG commercialized with the name of Nonex (for non–expanding) reducing lantern globe breakage by 60 %. Corning continued to explore BSG compositions and their applications [6–13].

In the US, "Pyrex" became synonymous with BSG after Joe Littleton from Corning Glass Works introduced it to the English speaking world in 1915. In 1922 the Pyrex glass production crossed the Atlantic and established in France. In 1930 it took part in the pharmaceutical World. The glorious success achieved with Pyrex baby bottles was experienced in 1936. In 1948 the electricity revolutionized people's cooking way. The glass manufacturing was progressively decreased in Bagneaux–Sur–Loing and the factory in Chateauroux quickly became the main manufacturing point in 1970. In 1975 it was the time of Pyrex tempered glass, not being scratched or oxidized and having everything to win from gaining over bakers. The official launch of the first range of glass freezer storage containers was made in 1985. In the years 2004–2010 the Pyrex brand added new materials (metal, ceramic and inox) to its offer. 2008–2014 were the years for the geographic expansion of the brand and the foreign markets normally led from France are now having new offices in Russia (2008) and Eastern Europe (2012) [14].

## 3. Brief Introduction to Boron

For centuries the only source of borax, $Na_2B_2O_5(OH)_4$, was Tibet's Lake Yamdok Cho deposits. In the year of 1808, Lussac and Thénard searching for in Paris, and Sir Davy in London, independently extracted boron by heating borax with potassium metal. Neither of them was successful in producing the pure element which is nearly impossible to achieve. In 1892 Moissan isolated a purer type of

Weintraub in the US had pure boron via sparking a mixture of boron chloride, $BCl_3$ vapor, and hydrogen [15].

To understand the BSGs one needs to register boron as a substance. Boron can be found in rocks, soil, and water. Earth crust has < 10 ppm boron with high levels found in the Western US and other regions from the Mediterranean to Kazakhstan. The average soil boron content varies from 10 to 20 ppm. Boron concentrations in rocks change from 5 ppm in basalts to 100 ppm in shales and averages 10 ppm in the Earth's crust overall. An average value of 4.6 ppm boron is present in seawater. Freshwaters normally range from < 0.01 to 1.5 ppm with higher concentrations in areas of high boron soil levels. Highly concentrated, economically sized boron mineral deposits, always in the form of boron compounds, are rare and generally exist in arid, volcanic and hydrothermal regions. Such deposits are being exploited in Türkiye, the US and various other countries. Borate mineral concentrates and refined products are manufactured, world widely sold and employed in a myriad of ways: in glass and related vitreous applications, in laundry bleaches, in fire retardants, as micronutrients in fertilizers as well as for many other purposes. Boron making trigonal and tetrahedral bonding leads to complexes with organic functional groups, many of which are biologically important [4].

## 4. Application Areas of Boron and Its Compounds

The most important application of amorphous boron is in the automobile airbags which are rapidly blown by gas in collusion and accepted as a security system. The relevant gas is generally N, appearing as a result of the degradation of sodium azidine ($NaN_3$). Such a reaction only takes place at high temperatures (> 300 $^oC$) and required energy is supplied by the use of amorphous boron with Na– or K–nitrate. Amorphous boron is also employed as a rocket fuel igniter and Na–octaborate is a flame retardant.

Amorphous boron is used in association with Ba–compounds in pyrotechnic flares with distinctive green color. But Ba–compounds are poisonous and have harmful effects on the living environment. According to recent studies made by an American military research group, it was reported that it is possible to use boron carbide replacing Ba in pyrotechnic mixture without losing a green color effect.
The isotope B–10 is good at absorbing neutrons, meaning that it could be employed for regulating nuclear reactors and plays a role in equipment for detecting neutrons. However, due to its mechanical weakness boron–containing steels or boron carbide are rather preferred.

Boron fibers (filaments) are used in plastic, resin (epoxy), metal or ceramic matrix composites for reinforcement. Those metallic matrices are Al, Mg, and Ti. Boron containing composite materials possess high–temperature strength, are light, flexible and easily workable. Boron filament reinforced composites are most importantly employed in the aviation industry. Additionally, they are also preferred in sport and leisure products (for example; tennis, racquetball, badminton rackets as well as fishing tackle, golf club, and skiing).

Boron is crucial for the cell walls of plants and thought to be harmful to animals. If used in higher concentrations it may disturb the metabolism of the human body. Some boron compounds are being investigated aiming to find out a possible treatment for brain tumors.

The most noteworthy boron compounds are boric acid ($H_3BO_3$), borax (sodium borate) and $B_2O_3$. Borax used to be employed for the preparation of bleach and as a food preservative [16].

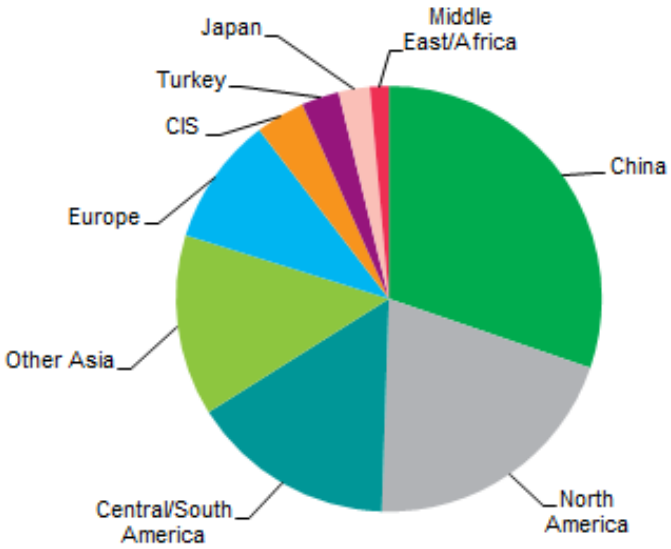


Figure 3. World consumption of boron materials and chemical–2018 [18].

Boron minerals are natural compounds possessing various levels of boric oxide in their structures. Ones generally found in Türkiye are tincal, colemanite, and ulexite, being primarily enriched by undergoing physical processes to achieve concentrated boron products, and then converted into various refined boron products through chemical processes.

Boron compounds are employed in various fields like glass, chemical and detergent industries, agriculture, ceramic and polymeric materials, metallurgy, nanotechnologies, automotive, energy, electronics and communications, space, aircraft and military vehicles, nuclear applications, fuels and construction (Figs. 3–4). Besides boron mostly consumed in the form of refined boron products, it could also be directly spent as concentrated boron products, approx. 80 % of which consumed in 2017 were employed in the glass, ceramic–frit, agriculture, and detergent–cleaning industries. The boron product consumption all around the world is nearly 4 million tons. About 59 % of World boron demand in 2018 was fulfilled by Türkiye [17].

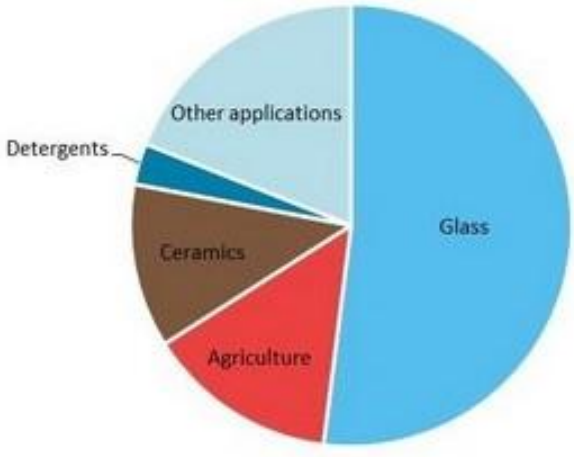


Figure 4. World boron minerals market by application–2019 [19]

## 5. Introduction to BSG

Although BSG was first largely employed in the production of kitchen glassware, thermometer glass, and railroad lanterns, at present very few companies are using it for such purposes, because of it's difficult production and high cost. Since the melting temperature of BSG is higher than that of other silicate glasses, it was more sophisticated to bring into industrial manufacture, and new techniques were needed. New burners, using oxygen and natural gas, have been developed. And for the most part, the production process stayed the same for the past 100 years or so. Thanks to its wide temperature range, strength, and chemical endurance borosilicate became "The Glass" of laboratories.

BSG consists of considerable levels of $SiO_2$ and $B_2O_3$ as major glass–forming oxides, and are typically made of 70–80 $SiO_2$, 7–13 $B_2O_3$, 4–8 $Na_2O$ or $K_2O$, and 2–8 $Al_2O_3$ (in wt. %). Glass having 7–13 wt. % $B_2O_3$ is recognized as low–BSG, and is majorly employed to manufacture chemical equipment, lamps, and tube envelopes. Glasses with 15–25 % $B_2O_3$ is classified as high–BSG, which is also grouped as leachable alkali–BSG having an optimum composition of 62.7 $SiO_2$, 26.9 $B_2O_3$, 6.6 $Na_2O$ and 3.5 $Al_2O_3$ (in wt. %). This glass could be further handled to manufacture the controlled pore glass being largely employed as a stationary median chromatography, or if needed, the pores could be closed up to give a clear impervious Vycor glass, commonly employed in cookware. The rise in $B_2O_3$ level, coupled with a very fine–scale secondary phase separation within the silica phase, improves the chemical endurance, and high–borate BSG considerably differentiates from low–borate ones [20]. In addition to ~75 % $SiO_2$ and 8–12 % $B_2O_3$, alkaline earth containing BSGs have up to 5 % alkali, earth alkali, and $Al_2O_3$. This subtype of slightly softer glasses (when compared to non–alkaline earth BSG) possesses $\alpha$ value changing between 4.0–5.0x$10^{-6}$/K and belongs to the chemically highly resistant group. $B_2O_3$ content for non–alkaline earth BSG is usually 12–13 % and silica level is above 80 %. High chemical endurance and low $\alpha$ (3.3x$10^{-6}$/K) make this a multi–talented glass [1].

## 6. Structure and Compounding of BSG

$B_2O_3$ is a glass former building a $B_2O_3$ glassy network. When suitable additions could be made into $B_2O_3$ then the structural rearrangement in the glass depends upon melting temperature or pressure and the interaction of the components in the chemical composition. Unlike silica tetrahedral structure, the initial modifier incorporation into $B_2O_3$–glass results in trigonal boron conversion to tetrahedral boron. Few or no non–bridging oxygen are formed. When alkali/earth alkali is inclined the tetrahedral boron starts converting back to asymmetric $BO_3$. In borate and silicate glasses being free of a modifier the structural units exist without mixing and once a modifier is incorporated then there will be overlap or mixing into one another. The alumina incorporation effect on the borate and borosilicate is to decline the amount of four–fold coordinated boron as $AlO_4$ formation first is more favorable. In $CaO–Al_2O_3–B_2O_3$ system $Al_2O_3$ and $B_2O_3$ compete for CaO to form $AlO_4$ and $BO_4$ units and $AlO_4$ is preferably formed before $BO_4$ because of higher single bond strength of the Al–O in $AlO_4$ as a comparison B–O bonds in $BO_4$. When alumina content increases the concentration of boron in $BO_4$ units decreases and the number of $BO_3$ units increases [21]. Fig. 5 presents Na–BSG from MD simulations [22].

Sastry and Hummel and later Galakhov and Alekseeva investigated the $Li_2O–B_2O_3–SiO_2$ system where compositions with less than ~20 mol % $Li_2O$ exhibited liquid–liquid phase separation, compositions with more than about 33 mol % $Li_2O$ indicated a strong crystallization tendency. Close to the boundary $Li_2O–B_2O_3$ the glass–forming tendency increases. Many workers studied the phase relationships in the $Na_2O–B_2O_3–SiO_2$ system. Morey, who has done the oldest work, reported that at atmospheric pressure no ternary–compound formation was indicated and the regions of the binary compounds were outlined

and isotherms determined. Skatulla, Vogel, and Wessel searched for metastable phase–separation phenomena in this system. Halter, Blackburn, Wagstaff, Charles, Schales and Wilkinsou conducted more recent researches on the metastable immiscibility surface in the system. Levin, McMurdie and Hall have given the phase diagram of the $CaO–B_2O_3–SiO_2$ system which exhibits a wide field of stable liquid–liquid phase separation. Phase relationships and the glass–forming areas in the $BaO–B_2O_3–SiO_2$ system were studied by Levin, Ugrinic, Hamilton, Cleek and Graner [1].

To understand the glass structure, knowing the coordination numbers and bonding type of the atoms, is extremely necessary. The character of atoms present primarily determines them. Variations in the glass structure also refer to the differences in their physical and chemical features. Aside from its scientific interest, structural work is also of vast technological importance. For examining the glass formation process one has to characterize the average product at various stages of this process. Knowledge of the correlations between the glass structure, composition and viscosity has crucial importance in terms of industrial manufacturing of all kinds of glass products. The current difficulty to describe the glass structure in detail has resulted in various approaches to explain the structure, 2 of which may be seen: the random–network and the crystallite hypothesis. In the former one, it is considered, for example, that the $SiO_4$ tetrahedra in vitreous silica are irregularly linked to one another. In the latter case, it is advised that in glassy silica sub–microscopically small regions with a regular structure exist and connected by regions with a disordered structure. Today, the crystallite hypothesis finds little support and the random network one is also in discussion [1].

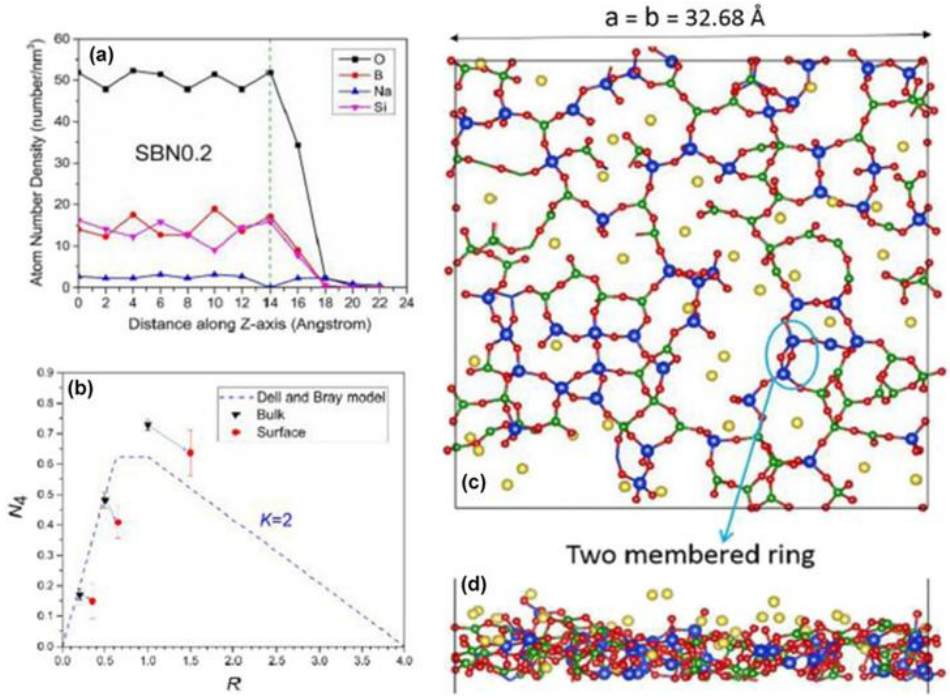


Figure 5. Na–BSG from MD simulations (Ren M., Deng L. & Du J.). Surface composition profile **(a)** and boron $N_4$ as a function of R (Soda to $B_2O_3$ ratio) for the bulk and surface **(b)**, surface structure of Na–BSGs: top view **(c)** and side view of top 5 Å **(d)** (reprinted with the permission from Ren M., Deng L. & Du J.) [22]

## 7. Properties of BSGs

### 7.1. Chemical endurance

BSG 3.3 has chemical durability to the attacks by nearly any product, making its endurance much more understandable. It is considerably durable against the attacks of deionized water, saline solutions, organic substances, halogens such as Cl and Br and most acids. Only a few chemicals (namely HF, concentrated phosphoric acid and strong caustic solutions) could cause noteworthy corrosion of the glass surface at higher temperatures. However, at ambient temperature, caustic solutions up to 30 % concentration can be easily handled by BSG. BSG could be categorized as follows:

| | |
|---|---|
| Hydrolytic durability (at 98 ºC) | Grain class ISO 719–HGB 1 |
| Hydrolytic durability (at 121 ºC) | Grain class ISO 720–HGA 1 |
| Acid endurance | Deposit of $Na_2O$ < 100 mg/dm² to ISO 1776 |
| Alkali endurance | Class ISO 695–A2 [23] |

**Acid attack**

The corrosion curves inhibit a maximum for different acids in the level ranging between 4 and 7 N. Additionally, the reaction speed diminishes considerably, therefore, the amounts of the eroded layer could be only a few thousandths of millimeter after some years. There is, naturally, a justification for referring to BSG 3.3 as an acid–resistant material [23].

**Alkali attack**

It could be noticed from the corrosion curves that the attack on the glass surface initially rises when the caustic solution concentration increases but beyond a maximum, it assumes a constant value. Increasing temperatures inclines the corrosion, while the reaction speed at low temperatures is so low that the reduction of the wall thickness is hardly noticeable over many years [23].

### 7.2. Physical features

The most important physical features for the plant construction can be followed below:

| | |
|---|---|
| Linear thermal expansion coefficient | $\alpha_{20/300} = (3.3 \pm 0.1) \times 10^{-6}\ K^{-1}$ |
| Thermal conductivity (between 20 and 200 °C) | $l_{20/200} = 1.2\ W\ m^{-1}\ K^{-1}$ |
| Specific heat capacity (between 20 and 100 °C) | $Cp_{20/100} = 0.8\ kJ\ kg^{-1}\ K^{-1}$ |
| Specific heat capacity (between 20 and 200 °C) | $Cp_{20/200} = 0.9\ kJ\ kg^{-1}\ K^{-1}$ |
| Density (at 20 °C) | $\rho = 223\ g\ dm^{-3}$ [23] |

**Thermal Expansion Coefficient**

BSG can be differentiated from other construction materials employed for process plants not only because of its well–known endurance against corrosion but also it's very low α value. To compensate for the thermal expansion caused by temperature changes there is no request for expensive measurements. This becomes of particular significance in the layout of long runs of glass pipeline. The linear measurement of BSGs is made to achieve some more qualitative knowledge on their structure. Value usually depends upon the temperature, composition, and thermal history of glass. Kumar et al. reported thermal expansion curves of Ca–BSGs [24].

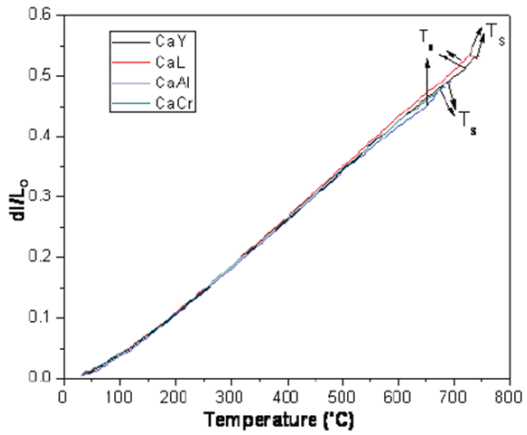


Figure 6. Thermal expansion curve of the as-prepared Ca–BSGs [24]

## Viscosity

The viscous features and melts structure are closely associated. Compositional variations reducing crossing–linking of the glass structure generally lower the viscosity, while those which rise connectivity incline the viscosity. Alkali borate and BSGs structures were largely searched mainly through NMR of $^{11}B$, $^{23}Na$, and $^{29}Si$. In the 1970s Yun and Bray proposed an original model. The composition–associated structural parameters K and R were recorded (where $K=[SiO_2]/[B_2O_3]$, $R=[Na_2O]/[B_2O_3]$). Mixed alkali BSGs exhibit a sophisticated relation of composition and structure. The sequence of polymerization of the silicate network and boron coordination is intensively dependent upon glass chemical composition. The effect of $Li_2O$ substitution on the strength of Si–O bonding and fraction of $[BO_3]$ and $[BO_4]$ have been studied.
Feng et al. have presented the viscosity data (Fig. 7) denoting the correlation between viscosity and temperature. The viscous variations of $Li_2O$ substitution depended upon $Li_2O$ content and temperature [25].

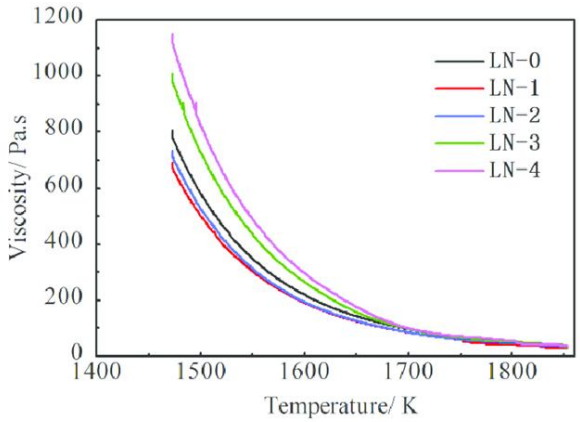


Figure 7. The viscosity of Na–BSGs concerning $Li_2O$ substitution from 1473 K to 1853 K [25]

## Electrical conductivity

Electrical conductivities and viscosities of solid glasses and melts are of great importance for a better comprehension of the temperature dependence of the structure and also for industrial melting

processes. Electrical conductivity is the feature of the greatest practical importance among the electrical properties. The strong change over large temperature ranges is of great interest [26].
BSG is non–conductive under normal temperatures and behaves as an insulator. The specific electric resistance of a monolithic BSG sample at 20 °C and in an environment being free of humidity is within the range of $10^{11}$–$10^{13}$ Ωm [27].

The electrical conduction in BSGs is based upon $Na^+$ ions transport through the glassy network. So, it should be dependent upon the mobile $Na^+$ ions concentration and their bond strength to the network. In silicate glasses, $Na^+$ ions are bonded to non–bridging oxygen. In BSGs, $Na^+$ ions prefer bonds to $BO_4$−groups with one bridging oxygen, which are stronger. This decreases the mobility of $Na^+$, thus the electrical conductivity, and increases the activation energy of the solid Na–BSG samples. According to Ehrt and Keding's study, the electrical conductivity of the Na–BSG is about three orders lower than that of the silicate glass (Na–silicate) with the same $Na_2O$ content, 15 mol %. With increasing temperature, the conductivity of Na–BSG approaches to that of Na–silicate, and at ~1000 °C the values are nearly the same. There is a remarkably strong increase of the activation energy and electrical conductivity in the temperature range above $T_g$, in the softening region. This increase is much stronger in Na–BSG than in Na–silicate glasses. The highest activation energy, ~2.8 eV, was measured for the NBS–B sample which has the lowest $Na_2O$ and high $B_2O_3$ content. The Eσ values decrease with increasing $Na_2O$ level. The electrical conductivity is strongly dependent upon $Na^+$ ions content and their mobility through the glassy network. Na–BSGs ($T \leq T_g$) have much lower electrical conductivity than Na–silicate glasses due to the special borate units. The $Na^+$ ions are more strongly bonded to $BO_4$−tetrahedra with bridging oxygen than to $SiO_4$−tetrahedra with non–bridging oxygen. Above $T_g$, in the softening region, the electrical conductivity of Na–BSGs increases strongly and approaches to the values of Na−silicate samples near 1000 °C. It is assumed that $BO_4$−units with bridging oxygen are transformed into $BO_3$−units with non–bridging oxygen which increases the electrical conductivity drastically. Different mechanisms are superimposed [26].

Stevens discussed the activation energy dependence of the electrical conduction upon the glass chemical composition, suggesting that the activation energy is sorted out by the average height of potential barriers. Beekenkamp employed electrical conduction measurements to examine the glass structure in the $K_2O$–$B_2O_3$–$Al_2O_3$ system. A fast rise of the conductivity is generally seen on the alkali oxide incorporation to vitreous silica up to ~20–30 mole % alkali oxide, at higher levels the increase is less mentioned. This rise in conductivity could be directly related to mobile alkali ions.

### 7.3. Mechanical Features

The permissible tensile strength of BSG 3.3 covers a safety factor, considering the practical experience on the glass behavior and, specifically, the fact of being a non–ductile material. Unlike other construction materials employed for similar purposes, it is not able to equalize stresses appearing at local disorders or flaws, as occurs in the case of metals which are ductile materials. Some properties are shown below and specified in EN 1595:

| | |
|---|---|
| Tensile and bending strength | K/S = 7 N $mm^{-2}$ |
| Compressive strength | K/S = 100 N $mm^{-2}$ |
| Modulus of elasticity | E = 64 kN $mm^{-2}$ |
| Poisson's ratio | n = 0.2 [23]. |

## 8. Application Areas of BSGs

BSG is mostly chosen for many usages. As well as laboratory items, BSG is employed to produce microwave glass cookware because of its heat resistance. That is why it is preferred to achieve high–quality beverage glassware, improving chemical endurance and dishwasher compatibility.

BSG is also employed in producing aquarium heaters, flashlights, guitar slides, high–intensity discharge lamps, etc. Besides, BSG possesses its usage in the semiconductor industry and in manufacturing the thermal insulation tiles of the famed Space Shuttle. Because of its high resistance and comparingly inert nature, BSG's are employed for the radioactive waste immobilization and disposal [28].

Many scientific lenses need a glass staying clear and strong under heat exposure. Borosilicate microscope lenses and microscope slides permit scientists to analyze tiny organisms and astronomers use them in telescopes.

It even became quite important in the arts. Stage lights can reach high temperatures during a 3–hour show. BSG is employed in both the spotlights that keep performers lit on stage and the flashlights that help them scurry around the set after the curtain falls. Glass sculptors and lampworkers use this "hard glass" to form everything from little artisan beads to huge museum exhibits [29].

Being resistant to high temperatures BSG becomes suitable for various applications such as heat and heat transfer, the manufacture of telescopes and other types of precision optics or the formation of high–powered lighting products, like LED lights and lights for the usage in the film industry. Boro glass is also ideal for hot mirrors, allowing for the reflection of IR light [30]. Glass is an inevitable material for modern life with the screens of mobile device, windows, for food and beverages bottles and jars, light–bulbs, solar arrays, microwave dishes, beakers, coffee pots, etc. (Fig. 8).

Solid glass microspheres (SGMs) supply multiple advantages like improved processing, perfect chemical endurance and heat resistance, thermal stability, low oil absorption, and are employed in automotive, electrical, household devices, adhesives, packaging, paint and construction sectors. When compared to other types of microspheres, like plastic or hollow glass, SGMs possess a high density, approximately 2.2 g/cc, for borosilicate, 2.5 g/cc for soda–lime, and 4.49 g/cc for barium titanate glass spheres. SGMs have high crushing strength making them suitable for high–stress applications where microspheres are exposed to lots of stress during processing or implementation [31].

The mobile phone with an extra transparent layer sitting on the actual liquid crystal display, the LCD screen, is an amazing piece of work. This layer is sensitive to touch and can convert the touch into an electrical signal, which the computer inside the phone can understand. As the screen grows larger, such as for TVs and other interactive displays like in banking machines and military applications, the resistive and capacitive type technologies for touch sensing quickly become less than adequate. It is more customary to use infrared touch–screens here. Although the infrared touch–screens are the most accurate and responsive, they are expensive and have other disadvantages. The failure rate is high because diodes used for generating the infrared rays fail often [32]. The security of the smartphone touch–screen has attracted considerable attention from academics as well as industry and security experts. The maximum–security of the mobile phone touch screen is necessary to protect the user's stored information in the event of a loss. Tahir et al. published a review paper, revealing that the most recent studies that propose new techniques for providing maximum security to smartphone touch

screens reveal multi–objective optimization problems [33]. Corning Company is producing highly mechanically resistant mobile phone and computer screens made of Gorilla Glass with superior visual quality [34]. Another well–known company, Schott, manufactures the products of electronic packaging, advanced optics, glass wafer and substrates, thin layer glass and highly transparent flat glass [35].

It must be pointed out that boron is also very crucial for textile fiberglass manufacture. The majority of them are employed in wind turbine blades, vehicles, and much more. While producing the glass and textile fiberglass, $B_2O_3$ plays a role of fluxing and network forming significantly lowers melting temperature, greatly facilitates processing, aids the fiberizing process and improves endurance in use. When they are employed in the applications of electronics or aerospace, borates are capable of controlling dielectric features–one reason is that textile fiberglass made with $B_2O_3$ is employed in the production of printed circuit boards, microelectromechanical systems, and thermal insulation tiles [36].

### 8.1. Aviation

**Airplane Exterior Lighting**

Throughout the long life of an aircraft, it will endure harm from harsh environments. There is no time for broken parts and repairs. For exterior lighting designs, borosilicate must be chosen and extend average time–on–wing. Unlike most polymer lenses, BSG is resistant to:

- UV degradation
- Chemical corrosion
- Abrasion from fine particulate
- Thermal stress

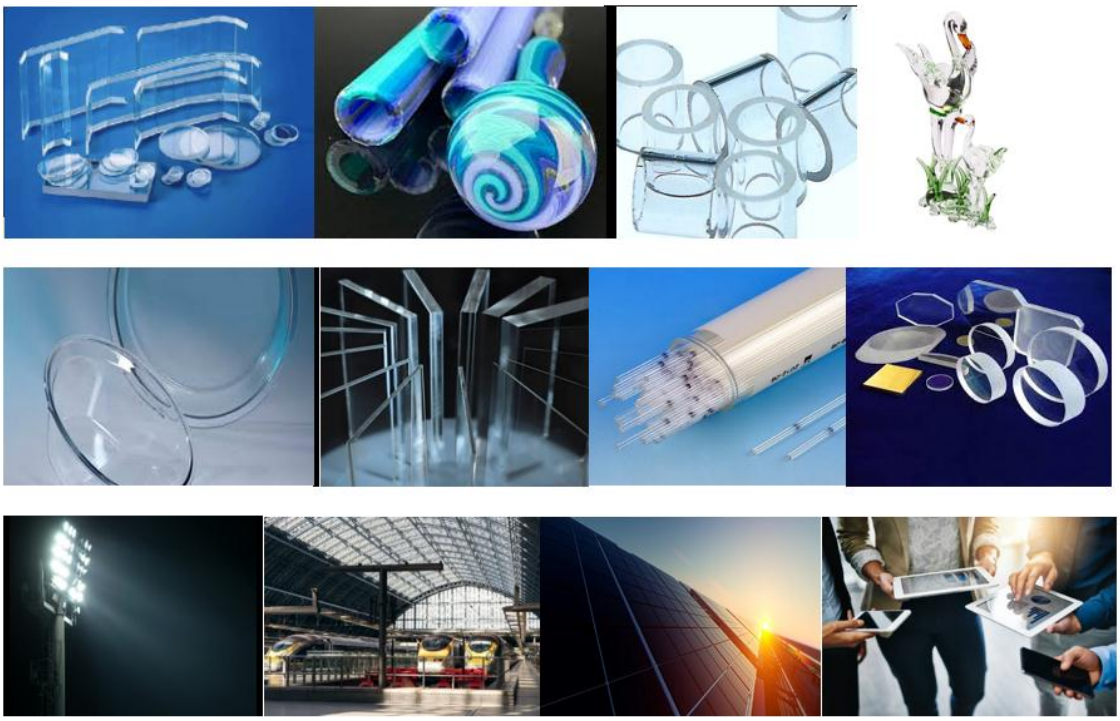

Figure 8. Some BSG products and usage areas [2, 30, 36–37]

For aircraft producers and operators, LED technology promises to keep planes operating longer with reduced maintenance costs and lower power consumption. The ability of pilots to see and be seen in poor weather conditions, especially on and near busy airfields, is critical to ensure public safety. Exterior aircraft lighting is a vital component helping provide necessary visibility.

To make sure a long lifetime and trustable performance, the lens covers employed in aircraft lighting applications have to supply consistent light transmission with minimal material degradation after being exposed to harsh conditions. Exterior aircraft lighting fixtures employ a transparent lens to cover and protect the light source with the most common lens materials being glass or plastic [38–39].

### Oxidation resistance and thermal shock features of self–healing SiCN/BSG–$B_4C$–$Al_2O_3$ coatings for C/C aircraft brake materials

Fan S. et al. deposited SiCN/BSG–$B_4C$–$Al_2O_3$ coating on carbon fiber–reinforced carbon matrix (C/C) brake materials to protect them from oxidation. Microstructural analysis inhibited that the coating was dense and uniform, depicting magnificent oxidation resistance and considerably low weight losses after oxidation in dry air for 10 h than SiCN/BSG–$B_4C$ coated samples. $B_4C$ is thought to react with the oxygen diffused into the coating to form $B_2O_3$ that could heal cracks of the coating and enhance its self–sealing ability and oxidation resistance.

Figure 9. Aircraft brake [41]

$Al_2O_3$ present in the outer glass layer is thought to exhibit the volatilization of $B_2O_3$, thereby reducing weight losses in the air. The fabricated coating also had superior oxidation resistance under fresh and seawater conditions with cracks and pores generated during the oxidization process being satisfactorily healed [40].

### Unmanned aerial vehicle (UAV) and missiles

Highly endurable materials like sapphire and AlON are the most enduring and abrasion–resistant, however, the costs are considerably higher when compared to glass. Additionally, sapphire and AlON cannot be molded. Sapphire and AlON must be grown, ground and polished; all are very time–consuming processes. In many applications, BSG is recommended (Figs. 10–11). This high-quality optical glass is satisfactory and could be molded, leading to the production thousands of times faster than processing sapphire type ones [42].

Figure 10. UAV [43]

Figure 11. Missile [44]

## 8.2. Optic

Optical borosilicate–crown glasses being virtually free of bubbles and inclusions have superior optical quality, uniform transmission in the visible, clear, colorless appearance, very high refractive index homogeneity and high purity of raw materials. They have typical usages such as demanding optical applications, the base material for precision optics, windows, lenses, prisms, substrates for mirror and filter coatings, measurement and sensor–technology usage and lenses and dispersion prims.
They can be formed in many shapes and comprised of a single element or form constituent parts of a multi–element compound lens system. Optical lenses are employed for focusing light and images, producing magnification, correcting optical aberrations and projection, mainly controlling the focus or divergence light employed in instrumentation, microscopy and laser applications (Fig. 12) [45–46].

Figure 12. Optical lenses [45, 47]

Many astronomical reflecting telescopes employ glass mirror components made of BSG thanks to its low value [48].

## 8.3. Optoelectronics

BSG wafers are largely employed for the process of anodic bonding of silicon with glass, so the silicon's thermal expansion is similar to these materials. BSG wafers have been developed for thin–film electronic circuits, requiring an extremely smooth surface with special electrical features. The general application of thin and ultra–thin BSG wafers is an electronic packaging of optoelectronic conductors.

BSG wafers are preferred in many industries, like the research and biomedical industry, because of its affordability (Fig. 13). They, in case of an explosion to high temperatures, manage to maintain clear and solid. The manufacturing applies the coating of indium tin oxide onto the surface, being transparent

in a visible spectrum that reflects the IR spectrum at the light source. Such technology is needed for protecting the insides of lenses, cameras, and film in projectors from the heat of the light sources [49].

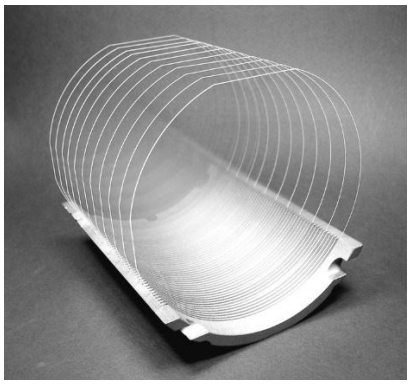

Figure 13. Glass wafers [49]

### 8.4. Nuclear waste immobilization

BSG's are worldwidely first chosen material for immobilizing high, low and intermediate–level wastes. Such a choice is based upon BSG flexibility in terms of waste loading and the capability to add many different types of waste elements, coupled with the good glass–forming ability, chemical endurance, mechanical integrity and superior thermal and radiation stability. The main constituent of BSGs is $SiO_2$ with relatively high $B_2O_3$, CaO, MgO, $Na_2O$ and $Al_2O_3$ levels and minor amounts of other oxides. $SiO_2$, $B_2O_3$, and $Al_2O_3$ have strong covalent bonds involving $SiO_4$, $AlO_4$, and $BO_4$ tetrahedra and $BO_3$ triangles [50].

Almost from the dawn of the nuclear age, mankind has had to face the problem of immobilizing highly radioactive nuclear waste. BSGs have inhibited that they possess a unique blend of processing and product features making them nearly ideal for this application [51].

### 8.5. Cover for a solar cell of EXOS–D

A borosilicate cover glass was developed for solar cells of the EXOS–D, a scientific satellite to be launched for the investigation of auroral particle generation. The composition of cover glass, designated BDX, is formulated to have an effective UV cut–off, which protects adhesives from deterioration and high radiation resistance, as well as high transmittance. All the cover glasses are coated with a conductive layer to keep an electrostatic isopotential on the satellite for accurate scientific measurements [52].

Solar collector tubes at power stations and solar water heating use collector tubes made of BSG to collect the reflected radiation for generating electricity. Specialized BSGs are also employed in photovoltaic cells thanks to their high impact resistance, compatibility, and strength to weight ratio (Fig. 14) [53].

Figure 14. Solar cells [53]

## 8.6. Health and Science

Laboratory glassware may be made from several types of glass, each with different capabilities and employed for different purposes. BSG is transparent and can withstand thermal stress. Borosilicate is largely employed in implantable medical devices like prosthetic eyes, artificial hip joints, bone cements, dental composite materials (white fillings) and even in breast implants (Fig. 15).

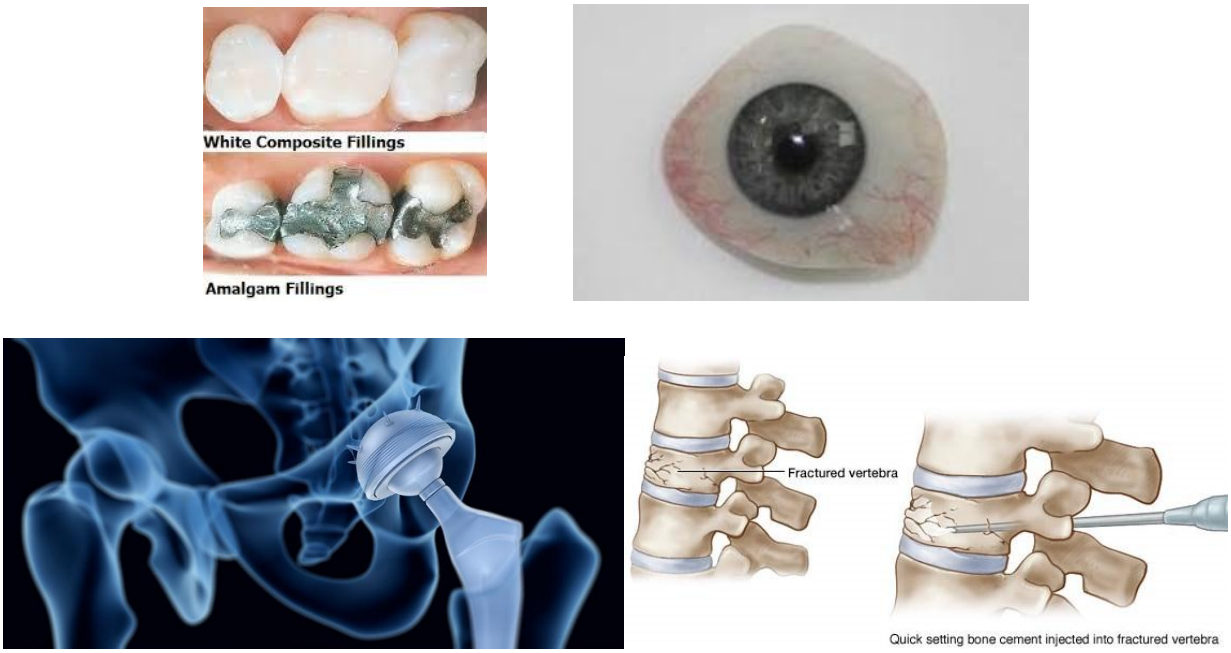


Figure 15. Applications of BSG in health and science [54–57]

## 8.7. Rapid Prototyping

BSG became the chosen material for fused deposition modeling or fused filament manufacture, build plates. When employed in combination with resistance–heating plates and pads, it's low value makes BSG an ideal material for the heated build platform, onto which plastic materials are extruded one layer at a time. The temperature, along with various coatings, ensure that the first layer may adhere and to stay adhered to the plate, without warping, as the first and subsequent layers cool following extrusion. The consequent residual stress formed when the plastic contracts as it cools, while the glass stays relatively dimensionally unchanged thanks to the low $\alpha$, supplies convenient assistance in removing the

otherwise mechanically bonded plastic from the build plate [58]. Fig. 16 presents a cycle of rapid prototyping.

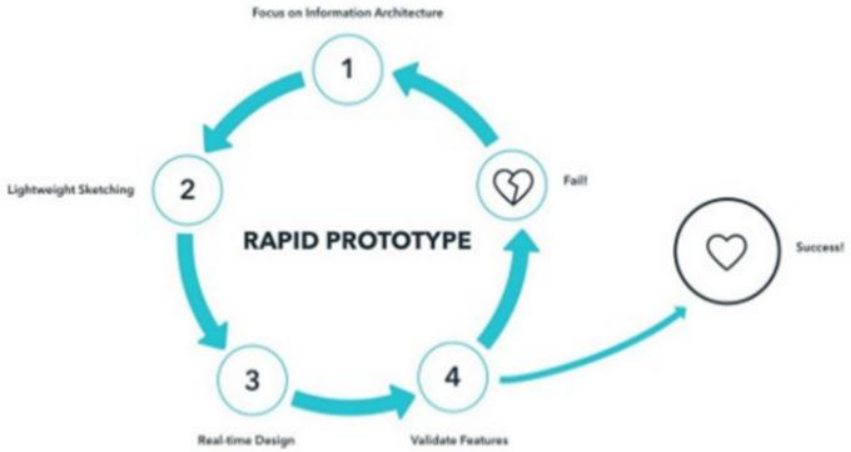


**Figure 16.** Rapid prototype [59]

### 8.8. Others

Aquarium heaters are sometimes made of BSG. Because of its high heat resistance, it can tolerate the significant temperature difference between the water and the heating element. Specialty glass smoking pipes for cannabis and tobacco are made from BSG. The high heat resistance makes the pipes more durable. Some harm reduction organizations also give out borosilicate pipes intended for smoking crack cocaine, as the heat resistance prevents the glass from cracking, causing cuts and burns that can spread Hepatitis C. BSG is also preferential for evacuated–tube solar thermal technology. BSG tubing is employed in specialty TIG welding torch nozzles replacing standard alumina nozzles. As a result, a clear view of the arc in situations where visibility is limited is allowed [58].

## 9. An Example of Manufacturing Process

The manufacturing process depends on product geometry.

### Floating

Molten raw materials → Fed to tin bath → Floating glass ribbon → Annealed and cut using a machine.

### Vello Process

olten glass flows from the tank past a rotating hollow mandrel. The tubing is mechanically drawn off. Air pressure through the mandrel and the rate of drawing affect diameter and wall thickness. The tubing is cut off to needed lengths and the end–fire–finished (Fig. 17).

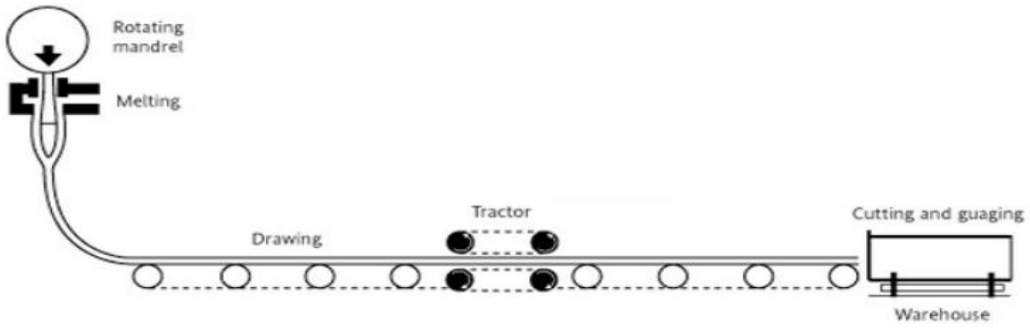


Figure 17. Molten glass flow chart [60]

**Molding**

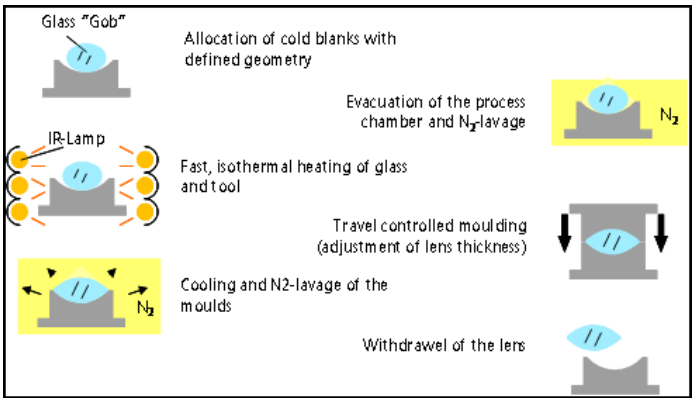


Figure 18. Precision glass molding is a process used for the production of high precision optical components from the glass without grinding and polishing [61]

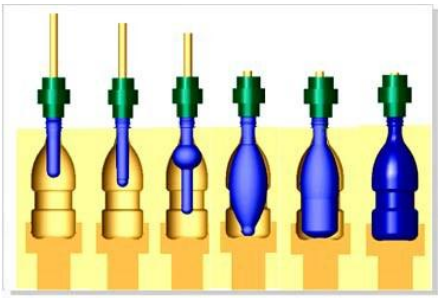

Figure 19. Molten glass which is collected in hollow pipes is expanded by blowing process through pipes [61]

## 10. Recent Developments

BSGs had been researched for years from many points of view. The development of batch for different applications, characterization, and recycling of technological glasses, etc. are mentioned below.
Xianghong et al. studied the wettability and interfacial reactivity between diamond and matrix [62]. Marzouk has reported that an increase of $Gd_2O_3$ concentration increases the elastic moduli, and Poisson's ratios lightly increase, which may cause an improvement in BSG acoustic properties [63]. The ballistic impact features of BSG (Pyrex) were worked using mild steel rods accelerated employing a light gas gun by Forde et al. [64]. Jacobs investigated the processing parameters' effects on material removal for BSG [66]. Variation of the chemical composition of ternary $CdS_{1-x}Se_x$ nanocrystals grown

in BSG was studied by Azhniuk et al. [66]. Geisler et al. searched for the textural, chemical, and $^{18}O$ and $^{26}Mg$ isotope tracer results from corrosion experiments with BSG [67]. To enhance the laser machinability of BSG, Matsusaka et al. doped Cu ions to the glass surface by an electric–field–assisted solid–state ion–exchange method [68]. Ghosh et al. investigated BaO addition influence on the thermal, crystallization, electrical and mechanical behavior of the Mg–La–Al BSG–ceramics [69]. The effect of Zr, Ti and Hf on the glass structure and the alteration kinetics of soda–lime–BSGs was studied by Bergeron et al. (Fig. 20) [70]. The researches of Bonfils et al. focused on a serial of BSGs of increasing chemical complexity [71].

A new fabrication process for epitaxial transfer of InP–based heterostructure barrier varactor diodes, as high–frequency varactor multipliers, onto low–dielectric BSG substrate, employing anodic bonding was presented [72]. Precipitation of nanoscale phases in a series of five related alkali–BSGs (with 4 mole % of $CeO_2$ and consist of varying levels of $Fe_2O_3$, $Nd_2O_3$, AgO, and $Cr_2O_3$) was examined by Yang et al. [73].

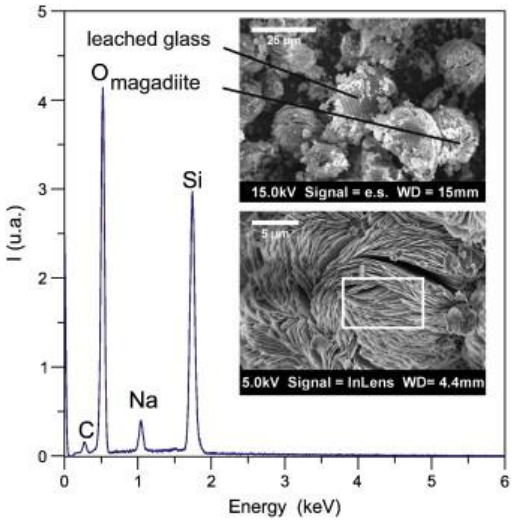


Figure 20. SEM pictures and EDS analysis of T1C4 glass powder leached at 90 °C, for 600 days. **(a)** Overview of the leached glass powder and the secondary crystalline phases. **(b)** Details of the secondary–phase morphology. EDS qualitatively confirms the magadiite ($Na_2Si_{14}O_{29}\cdot 11H_2O$) presence [70]

The Al–induced texturing method for glass sheets is applied to two types of glass used in the thin–film PV industry for superstrate modules: soda–lime glass and BSG in the study of Vayalakkara et al. [74]. The research paper of Dusserre et al. mainly concentrates on the development of an analytical method that permits extending the validity of the cylinder compression test (squeeze flow) over higher temperatures [75]. Reibstein et al. reported on Brillouin and in situ small–angle x–ray scattering (SAXS) analyses of topological heterogeneity in compressed Na–BSGs [76]. Separation of Pd from BSG–melt containing simulated high–level radioactive waste (Pd, Mo, Cs, Sr, Zr, Nd, Ni, Fe) using Sn as the solvent metal was studied, on lab–scale, by Hrudananda [77]. The behavior of Pu in the melter was evaluated employing paper works and corresponding analyses of DWPF melter pour samples by Bibler [78]. Rose et al. produced a simulated (inactive) borosilicate high–level waste (HLW) glass being on a full–scale vitrification line with composition simulating vitrified oxide fuel ($UO_2$) reprocessing waste [79]. In the research of Zhang et al., Si powder was incorporated into the diamond–BSG composites to enhance the oxidation resistance of diamond [80]. Bioactive Ca–titanate/BSG composites were developed by Villalpando–Reyna et al., indicating that these composites are potential

materials for bone tissue replacement and regeneration [81]. The ultrasonic velocities were measured in Ba–Pb–BSG samples of different compositions before and after irradiation with γ–rays by Laopaiboon et al. (Fig. 21) [82].

According to Toshihiko et al., it was clarified that the fatigue strength was enhanced by coating ceramic thin films on glass [83]. Kim et al. produced a Li–ion conducting glass, $Li_2O–B_2O_3–SiO_2$ through the conventional melt and quenching technique from a mixture of $Li_2CO_3$, $B_2O_3$ and $SiO_2$ powders [84]. Dharmadhikari et al. measured the refractive index change for a range of writing conditions as quantified in terms of energy dose [85]. A nano−structured $VO_2$ thin–film indicating a low metal–insulator transition temperature of 30 °C was manufactured via reactive ion beam sputtering followed by thermal annealing by Huang et al. This experiment paves the way of $VO_2$ thin film's application in smart windows [86].

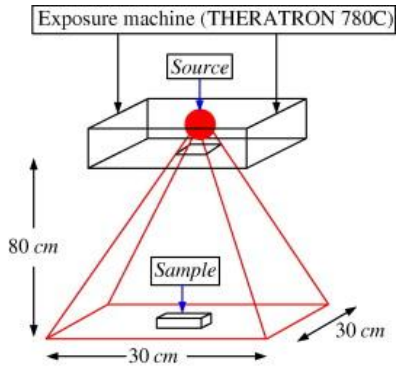


Figure 21. The geometrical arrangement of γ irradiation [82]

In the paper of Chillar, the standardization of PIGE methods for F determination using synthetic samples, and application to Ba–BSG samples were reported [87]. The ultrasonic velocity measurements for irradiated Bi–Pb BSGs $xBi_2O_3.(50–x)PbO.20B_2O_3.30SiO_2$ (x = 2, 4, 6, 8 and 10 mole %) were made at room temperature by the pulse–echo technique [88]. The crystal structure of two–phase and porous alkali BSGs with embedded magnetic atoms has been investigated employing XRD during the researches of Antropova et al. [89]. As Hamodi et al. mentioned in their work, the interaction led to the formation of a monocrystal SiC, dispersed in vitreous silica as a crystalline inclusion [90]. The study of Hamodi et al. demonstrated comprehensive experimental and analytical works and exhibited that it was possible to minimize the volume of the waste while keeping the required safety levels [91]. The bandgap of the glass was studied by Du et al. [92]. In the paper of Hao et al., Zn–BSGs ($ZnO–B_2O_3–SiO_2$) were added to $Ba_{0.3}Sr_{0.7}TiO_3$ (BST) ceramics to sort out the role of glass additives on the dielectric features and energy storage density of BST [93].

The effect of concentration and structural factors on the character of the temperature dependence of the glass viscosity in the $K_2O–B_2O_3–SiO_2$ and $Na_2O–B_2O_3–SiO_2$ systems within the range of $10^9$–$10^4$ Pa sec was determined by Levitskii et al. [94]. IR spectroscopy was used to study the behavior of water in model glasses of the $Na_2O–B_2O_3–SiO_2$ and $K_2O–B_2O_3–SiO_2$ systems [95]. Understanding of dissolution processes of BSGs can shed light on mechanisms of degradation of nuclear waste forms according to the research paper of Zapol et al. [96]. Ahamed et al. reported the development of a deep plasma etching process for FS and BSG employing magnetic neutral loop discharge plasma. The experiment design with etching parameters and variation in masking materials supplies a systematic approach to the manufacture of sensors, resonators, and microsystems using fused silica and BSG [97].

Radiation effects on BSG induced by 0.5 MeV He ions and 1.2 MeV electrons have been investigated by nanoindentation and Raman measurements in the study of Yang et al. [98].

Understanding the role of $V_2O_5$ within BSG matrices is vital for developing novel matrices toward immobilization of sulfate–containing high–level nuclear wastes according to Sengupta et al. [99]. In the paper of Lai et al., by employing the colloidal probe technique, the interaction forces between glass and cellulose material were investigated [100]. Synthesis and structural features of Pb–Sr titanate BSGs with the incorporation of chromium trioxide and graphene nanoplatelets were examined by Gautam et al. [101]. The development of photonic crystal fibers made of two or more types of glasses can be of considerable advantage in designing specific features of photonic crystal fibers (Fig. 22) [102]. The mass attenuation coefficient, effective atomic number, and electron density were measured in the composition of Bi–Na–Ca borosilicate at different concentrations (x = 0, 5, 10, 15, 20 and 25 mole %) [103]. The equipment and procedure for the fabrication of magnetic alkali–BSGs by the method of induction melting were studied by Naberezhnov et al. [104].

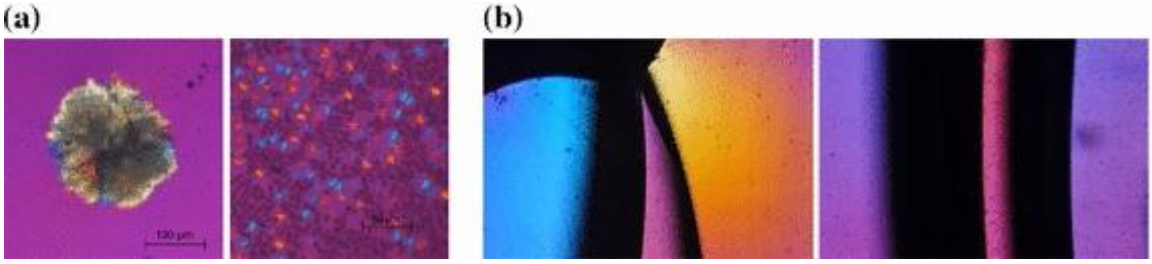


Figure 22. (**a)** Examples of the crystallization on the surface of the glass sample and (**b)** stress induced by the thermal expansion difference (polariscopic images) [102]

During the firing of the screen–printed Ag contacts in industrial crystalline Si solar cells, an interfacial glass layer is formed between the Ag bulk contact and the Si substrate. The conduction mechanisms across the interfacial glass layer, which consists of Pb–BSG enclosing Ag colloids was investigated utilizing numerical modeling. Mackel et al. revised the characteristics of applications that employ similar glasses, such as photodetectors, thick–film transistors, and surface passivation [105]. Kilymis et al. made the classical molecular dynamics simulations to investigate the changes under compression in the local and medium–range structural features of three Na–BSGs with varying Na content [106]. Barlet et al. searched for the mechanical response of Na–BSGs as a function of their chemical composition (Fig. 23) [107]. Three BSG ($SiO_2$–$B_2O_3$) fixed charge potentials from the literature are compared and their suitability for the usage in simulations of radiation damage is assessed. For a range of densities, Jolley et al. generated glass structures by quenching at $5\times10^{12}$ K/s using constant volume molecular dynamics [108].

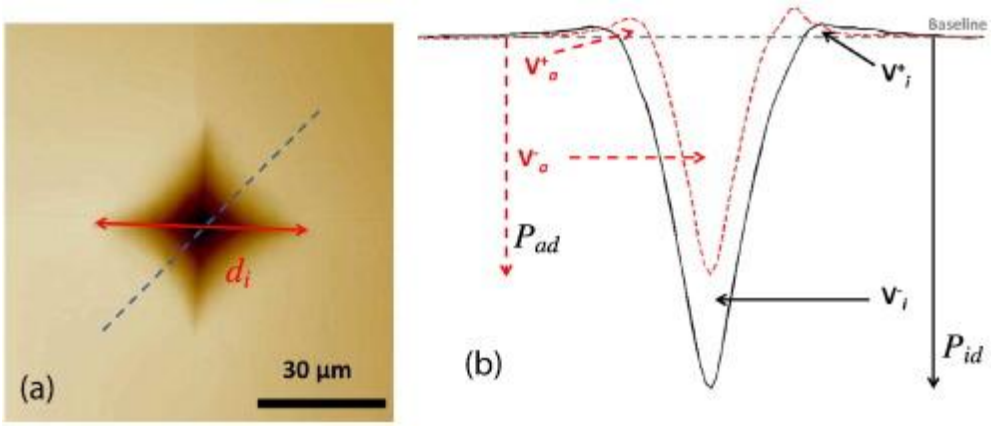


Figure 23. (a) A typical indentation imprint used for determining the indentation diagonal length, ($d_i$ and marked by a continuous line) and for estimating the pile–up profile (dotted line). (b) Sketch indicating the evolution of indentation prints before (black solid line) and after annealing (red dotted line). $V^+$ and $V^-$ exhibit the volume above and below the baseline (grey dotted line), respectively [107]

Na–borosilicate (NBS) and Ba–Na–borosilicate (BNBS) glasses employed for immobilization of high–level nuclear waste undergone to leaching experiments under hydrothermal conditions in an autoclave at 200 °C for differing time. Characterization studies have confirmed that, upon leaching, an aluminosilicate phase formation, Zeolite–P ($Na_6Al_6Si_{10}O_{32}.12H_2O$), appears with NBS glass [109]. BSG waste used as a cement additive could improve its radiation shielding according to Weiwei et al. [110]. The measurements of the CLTE and relative elongation of two types of BSGs–LK5 and Borofloat 33–were analyzed by Sinev et al. [111]. Alkali–BSGs constitute a current standard as structural elements for producing neutron guides. Such optical devices are commonly installed in large neutron research facilities to enable the transport of moderated neutrons from an intense source to scientific instruments. However, this equipment is known to suffer mechanical degradation arising from irradiation due to the neutron transport written in the paper of Boffy et al. [112]. Effects of Nd content on structure and chemical durability of zirconolite–Ba–BSG–ceramics was discussed by Wu et al. [113]. Na– and Ba–BSGs having various levels of $Al_2O_3$ were prepared by the conventional melt–quench method and their structural information was achieved by $^{29}Si$, $^{11}B$ and $^{27}Al$ magic angle spinning nuclear magnetic resonance technique in the works of Dhara et al. [114]. The arrayed micro–bumps are a new finding, and they might be employed to change the surface features. Bump formation is caused by phase separation, and volume swelling is induced by ion irradiation according to the studies of Wang et al. (Fig. 24) [115]. XANES analysis of a Cm–doped BSG was done under a self–irradiation effects by Bouty et. al. [116]. Structural analysis depicted that at higher temperatures the Na–borosilicate liquid does not have a specific structure according to Mylvaganam et al. [117].

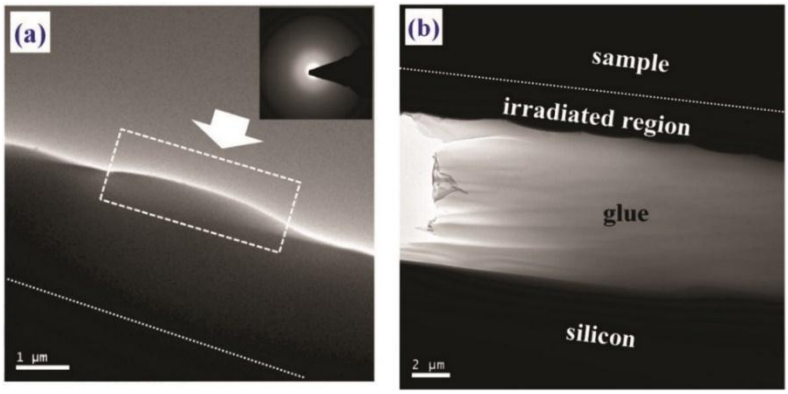


Figure 24. The TEM image of the Xe ion irradiated glass at $9.0 \times 10^{15}$ ions.cm$^{-2}$ [115]

Rathnaraj et al. gave a new approach to waste glass recycling LM6 metal matrix composite with BSG reinforcement for aerospace applications [118]. The mixed modifier effect in the Li–Ca–BSGs having a composition of $0.4[(1x)Li_2O–xCaO]–0.6[(1y)B_2O_3–ySiO_2]$ with x in the range of 0~1 and y in the range of 0.33~0.83 was worked by Shih et al. [119]. The application of BSGs as transparent armor materials has led to various fundamental studies on the structural and mechanical behavior of these materials under a variety of strain–rate loading conditions to better understand their high pressure, hydrostatic, and multiaxial responses; in addition to the associated failure mechanisms [120]. The surface plays an important role in the physical and chemical features of oxide glasses and controls the interactions of these glasses with the environment, thus dominating features like the chemical durability and bioactivity according to the studies of Ren et al. [121]. X–ray tomography of feed–to–glass transition of simulated borosilicate waste glasses was worked by Harris et al. [122]. BSG is largely employed in advanced industrial technology beside in medical applications. The brittleness and hardness are the main constraints of BSG, because of these features it is very difficult to machine it by conventional and non–conventional machining process. The various experimental researches in the field of BSG have been in detail reviewed and presented in a tabulated format which will useful for quick referencing [123]. In the study of Talimian et al. they investigated the effects of the electric field–assisted ion exchange (EF–IE) on K for Na ion exchanges of soda–borosilicate and SLS glasses [124].

Del Cerro et al. reported their latest results on the development of BSGs with persistent luminescence (PeL) [125]. Meier et al. investigated the impact of different oxygen concentrations during boron diffusion at 950 °C using BSG layers deposited by atmospheric pressure chemical vapor deposition (CVD) [126]. The influence of $S_{53}P_4$–based BSGs and glass dissolution products on the osteogenic commitment of human adipose stem cells were studied by Ojansivu et al. [127]. The formation of molecular oxygen was seen in BSGs irradiated with energetic ions and electrons, having significant effects on mechanical features of glasses and evaluation of high–level nuclear waste immobilization [128]. Mihailetchi et al. presented a passivation method of the $p^+$–doped areas by employing this in situ grown $SiO_2$ in combination with a plasma–enhanced–chemical–vapor–deposited $SiN_x$ layer [129]. Soliman et al. investigated thermoluminescence characteristics and dosimetric parameters of $Nd^{3+}$–doped alkali BSG [130]. The black TiAlN decorative film was prepared on the BSG by the magnetron sputtering in equipment with multiple vacuum chambers by Jinlong et al. [131]. Pressure excited densification and compression of a reprocessed sample of BSG were searched for by x–ray radiography and energy–dispersive XRD by Ham et al. [132]. The reprocessing of a commercial BSG was conducted by cyclical melting and cooling [133]. The release of therapeutic ions during dissolution is requisite for the success of bioactive glasses in medical applications. Therefore, different borate and

BSGs undoped and doped with Cu or/and Zn based on the 13–93 composition were tested and compared to the well–known 13–93 bioactive glass in several dissolution media (Fig. 25). The dissolution rates varied following the trend of borate glasses > BSGs > silicate glasses [134].

Figure 25. Doped bioactive glass micro view [134]

Effects of radiation damage and composition on phase separation in borosilicate nuclear waste glasses were studied by Patel [135]. Ham et al. investigated pressure-induced densification and compression of a reprocessed sample of BSG by x–ray radiography and energy–dispersive XRD [136].

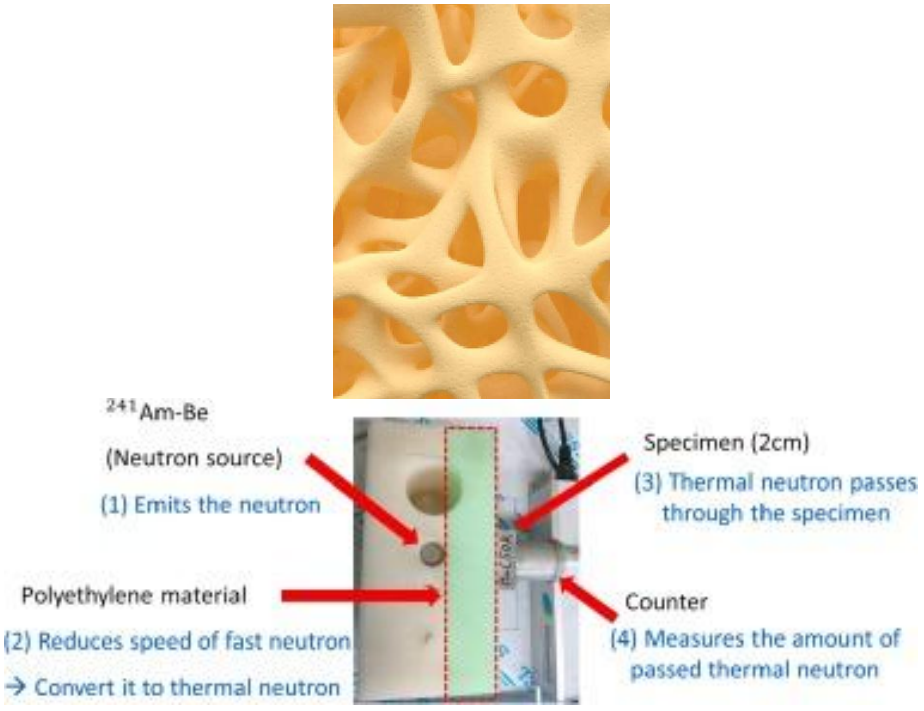


Figure 26. An experimental setup for thermal neutron shielding measurement [137]

In the work of Lee et al., BSG was employed as a form of mineral additive and fine aggregate to produce neutron shielding mortar (Fig. 26) [137]. Based on molecular dynamics simulations, Wang et al. investigated the atomic structure of a series of BSGs and indicated that the network–modifying cations show some level of clustering depending upon composition–in a good agreement with Greaves' modified random network model [138]. The effect of cerium oxide on the thermal features and the glass structure has been studied for the $Li_2O$–($Na_2O$–$K_2O$)–$B_2O_3$–$SiO_2$ system by Eremyashev et al. [139].

Zn–BSGs and regarding glass–ceramics in the $55ZnO.25SiO_2.20B_2O_3$ system (mole %) containing various amounts of MnO have been made by Abdel–Hameed et al. [140]. Potential–induced degradation was examined in small–size Cu (In, Ga)$Se_2$ (CIGS) sub–modules of individual cells [141]. Differences in radiation effects of Na–BSG and vitreous silica with ions were studied by Guan et al. [142]. The mechanical feature changes in 3 types of BSGs induced by 8.0–MeV $Au^{3+}$ have been investigated via nanoindentation measurements [143]. To increase the sulfate solubility in the glass matrix, barite−BSG–ceramics were proposed and prepared through a melt quenching method by Wu et al. [144]. Na−BSGs are candidate materials for high–level radioactive waste vitrification; therefore,

comprehending the irradiation effects in model BSG is crucial. Effects of electronic energy deposition and nuclear energy deposition induced by the impact of heavy ions on the hardness and Young's modulus of Na–BSG were examined by Du et al. [145]. Mo is a fission product with high fission yield, being present in high–level liquid waste (HLW). Presently HLW is confined in BSG matrix. To improve the solubility of $MoO_3$, different host glass matrices containing different amounts of $MoO_3$ were prepared and investigated. Phosphate bearing BSG exhibited increased solubility for $MoO_3$ [146]. Roldán Del Cerro et al. reported their latest results on the development of BSGs with persistent luminescence (PeL) [147]. The borate structural variations along with $Dy_2O_3$ presence decreased both the UV transmission and the optical energy gap, increased the refractive index and created several transitions at different wavelengths according to Shaaban et al. [148]. The results of AC conductivity may show the dominance of electronic conduction over the ionic transfer in the studied samples of Morsi et al. [149]. To determine the source of molecular oxygen in irradiated BSGs, several oxygen atoms were artificial randomly removed from the pristine glasses by molecular dynamics simulation in the study of Yuan et al. [150]. In the paper of Weigel et al., different BSG and aluminosilicate glasses are compared concerning their etching behavior [151]. Radiation effects on BSG have been extensively studied by Guan et al. [152]. Abdel–Hameed et al. characterized the effect of MnO addition and heat treatment on phase formation, microstructure and photoluminescence features of the glasses and glass–ceramics [153] The ion– and electron irradiation–induced mechanical feature changes of NBS glasses were compared by Lv et al. [154]. Effect of Ce, as a surrogate for actinide elements, on structure, crystallization kinetics, glass transition kinetics and water–resistance of the studied BSG was examined by Zhu et al. [155]. Glass, which was initially used for the protection of driver and passengers from outside effects, has been an important part of most researches and new properties have been added, thus its usage fields have enlarged. Moreover, through new production technologies, other materials with glassy properties have become an inevitable part of the automotive industry. Karasu et al. published a review paper on this issue (Fig. 27) [156].

Figure 27. Glass parts used in automobiles [156]

## 11. Conclusions

From its first invention in 1893 to the present time BSG has giant steps from both scientific and technological points of view. Thermometer glass, laboratory glass, and lamp chimneys were the first fields of application for chemically and thermally resistant BSG. Thanks to its wide temperature range, strength, and chemical endurance borosilicate became "The Glass" of laboratories. When the time passes application spectrum of BSGs enlarged: our daily life mobile device–screens, windows, bottles, and jars for food and drink, lightbulbs, solar arrays, drinking glasses, cosmetics jars, microwave dishes, test tubes, and beakers, coffee pots, laboratory items, aquarium heaters, flashlights, spotlights, guitar slides, high–intensity discharge lamps, printed circuit boards, microelectromechanical systems, the thermal insulation tiles for space shuttles, immobilization and disposal of radioactive waste,

microscope lenses and microscope slides to analyze tiny organisms, telescopes and other types of precision optics hot mirrors, and biomaterials, fiberglass for electronics or aerospace applications and textile fiberglass. Researches on BSGs, being one of the inevitable materials for everybody, and their potential application fields are still intensively carried out as in the past, present time and inevitably in the future, facilitating human life.

**References**


[1]. Konijnendijk W. L., The structure of borosilicate glasses, Technische Hogeschool Eindhoven, 1975, DOI: 10.6100/IR146141.

[2]. https://www.google.com/search?q=application+of+borosilicate+glasses&sxsrf=ACYBGNTQ7F6wtgjb4LLr-DG1gXI4F1NCXA:1576845618438&source=lnms&tbm=isch&sa=X&ved=2ahUKEwjWjc_Xn8TmAhWYTBUIHR5ZBuwQ_AUoAnoECBAQBA&biw=1707&bih=850&dpr=1.5#imgrc=_ (Access Date: 20.12.2019).

[3]. https://www.google.com/search?q=books+on+borosilicate+glass&tbm=isch&source=univ&sa=X&ved=2ahUKEwja0KrbppnmAhXUiVwKHXiEBrEQsAR6BAgKEAE&biw=1707&bih=801 (Access Date: 19.12.2019).

[4]. Woods W. G., An introduction to boron: History, sources, uses, and chemistry, Environmental Health Perspectives, 1994, 102 (7): 5–11.

[5]. https://www.chemeurope.com/en/encyclopedia/Borosilicate_glass.html (Access Date: 25.12.2019).

[6]. Travis N. J., Cocks E. J., The tincal trail–A history of borax, London: Harraps Ltd., 1984.

[7]. Steiner J., Schott O., The invention of borosilicate glass, June 1993.

[8]. Steiner J., Glastech. Ber., 1993, 66: 165.

[9]. Vogel W., Chemistry of glass, Amer. Ceram Soc., Columbus, OH, 1985.

[10]. Varshneya A. K., Mauro J. C., Fundemantals of inorganic glasses, 3rd Edition, Elsevier, 2019.

[11]. https://www.environmental-expert.com/articles/borosilicate-glass-a-brief-history-61745 (Access Date: 19.12.2019).

[12]. https://www.kaufmann-mercantile.com/field-notes/post/793/borosilicate-glass, (Access Date: 09.07.2019).

[13]. Anonymous, Eugene Cornelius Sullivan–Glass Scientist, Corning Glass Works, Corning, NY, 1964.

[14]. https://www.pyrex.eu/pages/our-history (Access Date: 25.12.2019).

[15]. https://www.rsc.org/periodic-table/element/5/boron (Access Date: 19.12.2019).

[16]. Yünlü K., Boron compounds, synthesis methods, properties and applications, BOREN (National Boron Research Instituete) publication supported by T.R. Ministry of Natural Sources, İstanbul, 2016 (in Turkish).

[17]. https://enerji.gov.tr/en-US/Pages/Boron%20 (Access Date: 19.12.2019).

[18]. https://www.google.com/search?q=boron+usage+areas+of+the+world&tbm=isch&tbs=rimg: (Access Date: 25.11.2019).

[19]. Boron minerals: 2019 World market review and forecast to 2028, July 2019, https://mcgroup.co.uk/researches/boron (Access Date: 27.11.2019).

[20]. Hasanuzzaman M. et al., Properties of glass materials in Reference Module in Mater. Sci. and Mater. Eng., Elsevier, 2016.

[21]. Grema L. U., PhD Thesis, The University of Sheffield, 2018.

[22]. Du J., Rimsza J., 2017, DOI: 10.1038/s41529-017-0017-y.

[23]. https://za.dedietrich.com/products-solutions/borosilicate-glass-properties (Access Date: 19.12.2019).
[24]. Kumar V. et al., Phys. Chem. Glasses: Eur. J. Glass Sci. Technol. B, October 2011, 52 (5): 212–220.
[25]. Fe H., Physics Procedia, 2013, 48: 73–80.
[26]. Ehrt D., Keding R., Phys. Chem. Glasses: Eur. J. Glass Sci. Technol. B, 2009, 50 (3): 165–171.
[27]. Lima M. M. R. A. et al., J. of Alloys and Compounds, 2012, 538: 66–72.
[28]. http://www.borosil.com/an-overview-of-borosilicate-glass/ (Access Date: 30.12.2019).
[29]. http://www.qorpak.com/pages/whatisborosilicateglass (Access Date: 19.12.2019).
[30]. https://www.swiftglass.com/blog/borosilicate-material-focus (Access Date: 20.12.2019).
[31]. Karasu B. et al., Glass microsperes, El–Cezerî Journal of Science and Engineering, 2019, 6(3): 613–641.
[32]. https://www.westfloridacomponents.com/blog/how-does-the-touch-screen-work/ (Access Date: 24.02.2020).
[33]. Tahir M. I. et al., Computers & Security, August 2019, 85: 1–24.
[34]. https://www.corning.com/gorillaglass/tr/tr.html (Access Date: 24.02.2020).
[35]. https://www.schott.com/english/applications/communication_electronics.html (Access Date: 24.02.2020).
[36]. https://www.borax.com/applications/glass-textile-fiberglass (Access Date: 20.12.2019).
[37]. https://www.google.com/search?q=usage+areas+of+borosilicate+glasses&sxsrf=ACYBGNSYsdBpwui5tMllym3KjBwmfdX7sQ:1576846624811&source=lnms&tbm=isch&sa=X&ved=2ahUKEwiApL-3o8TmAhXRRBUIHReyAQ8Q_AUoAXoECA4QAw&biw=1707&bih=801&dpr=1.5#imgrc=UvxrGy0RCaocXM: (Access Date: 20.12.2019).
[38]. Lombardo D., Aircraft systems, 2nd Edition, Blackclick, US, McGraw Hill Professional Publishing 2000.
[39]. https://www.led-professional.com/resources-1/articles/abrasion-in-transparent-lens-materials-for-exterior-aircraft-lighting (Access Date: 25.12.2019).
[40]. Fan S. et al., Ceram. Int. , 2019, 45 (1): 550–557.
[41]. https://www.google.com/search?sxsrf=ACYBGNRAWHBxiL8vOcy4WGNTpHN92xtFhw:1577290303925&q=aircraft+brake&tbm=isch&source=univ&sa=X&ved=2ahUKEwjRppeimNHmAhW0unEKHbkSAdMQsAR6BAgBEAE&biw=1707&bih=850 (Access Date: 25.12.2019).
[42]. https://rayotek.com/aerospace-aviation-molded-optical-glass-domes.htm (Access Date: 25.12.2019).
[43]. https://www.google.com.tr/url?sa=i&rct=j&q=&esrc=s&source=images&cd=&cad=rja&uact=8&ved=2ahUKEwiK8P7e-IHiAhWBZ1AKHW0dCWIQjRx6BAgBEAU&url=http%3A%2F%2Fwww.airbus.com%2Fdefence%2Fuav.html&psig=AOvVaw2gpxGFEpuEVRRZR-FQa0NG&ust=1557061562903452 (Access Date: 25.12.2019).
[44]. https://www.armytimes.com/resizer/xFqOYZdi9iSrLR9uz3Tg6cLGGns=/1200x0/filters:quality(100)/arc-anglerfish-arc2-prod-mco.s3.amazonaws.com/public/FZIYQ2FPRJG5ZJQLZLDAURTZRY.jpg (Access Date: 25.12.2019).
[45]. https://www.pgo-online.com/intl/BK7.html (Access Date: 26.12.2019).
[46]. https://www.uqgoptics.com/catalogue/lenses/ (Access Date: 26.12.2019).
[47]. https://www.google.com/search?q=optical+lens&sxsrf=ACYBGNS0gJOeFytmaYgRK49

WqeQO4JAtvw:1577291271295&source=lnms&tbm=isch&sa=X&ved=2ahUKEwjYgLvvm9HmAhWqVRUIHdPXB7MQ_AUoAXoECA4QAw&biw=1707&bih=850 (Access Date: 26.12.2019).
[48]. Tobin V., Evolution of the Foucault–Secretan reflecting telescope, J. of Astronomical History and Heritage, 2016, 19 (2): 106–184.
[49]. https://nanografi.com/blog/borosilicate-glass-wafers/ (Access Date: 26.12.2019).
[50]. Ojowan M. et al., Immobilisation of radioactive wastes in glass in An Introduction to Nuclear Waste Immobilisation, 3rd Edition, 2019.
[51]. Plodinec J., Glass Techn., 2000, 41 (6):186–192.
[52]. https://www.researchgate.net/publication/241400793_Borosilicate_cover_glass_for_solar_cell_of_EXOS-D (Access Date: 26.12.2019).
[53]. https://www.ceramicindustry.com/articles/97561-borosilicate-glass-continues-to-dominate-demand-for-anhydrous-borax (Access Date: 26.12.2019).
[54]. https://www.whitemarshdental.com/wp-content/uploads/2015/07/white-fillings-1-1.jpg (Access Date: 26.12.2019).
[55]. https://www.google.com/search?q=prosthetic+eyes&sxsrf=ACYBGNSNMz63EJRRoaOqMh5wly1V4IGCYA:1577350036917&source=lnms&tbm=isch&sa=X&ved=2ahUKEwiQ84vl9tLmAhWmURUIHcfnCjEQ_AUoAXoECBIQAw&biw=1707&bih=801&dpr=1.5#imgrc=_(Access Date: 26.12.2019).
[56]. http://4.bp.blogspot.com/-8cB0MRUQnws/VpL44mXQVTI/AAAAAAAAAEA/7BYkWwkHv2E/s640/Vertebroplasty2.jpg (Access Date: 26.12.2019).
[57]. https://www.google.com/search?q=borosilicate+glass+in+dentistry&sxsrf=ACYBGNQzD--n5r0jEPOKHAJdaoQxoV57HA:1577349362726&source=lnms&tbm=isch&sa=X&ved=2ahUKEwj2wc6j9NLmAhWBonEKHVtVDHUQ_AUoAXoECAsQAw&biw=1707&bih=801&dpr=1.5#imgrc=zrmRlRpl536jNM: (Access Date: 26.12.2019).
[58]. https://en.wikipedia.org/wiki/Borosilicate_glass (Access Date: 26.12.2019).
[59]. https://image.slidesharecdn.com/rapidprototyping2-161004194933/95/rapid-prototyping-20-18-638.jpg?cb=1475610668 (Access Date: 26.12.2019).
[60]. https://www.eurotherm.com/en/glass-manufacturing-applications/tube-glass/ (Access Date: 26.12.2019).
[61]. https://tue.iitm.ac.in/Teaching_and_Presentation/grouppresentations/2016/Instrumental%20technique%2014-5-16%20Sugi.pdf (Access Date: 26.12.2019).
[62]. Xianghong Z. et al., Elsevier, 2010, DOI: 10.1016/j.ijrmhm.2009.10.008.
[63]. Marzouk S. Y., Physica B: Condensed Matter, 2010, 405 (16): 3395–3400.
[64]. Forde L. C. et al., Int. J. of Impact Eng., 2010, 37 (5): 568–578.
[65]. Jacobs S., Applied Optics, 2010, 49:10.
[66]. Azhniuk Y. M. et al., J. of Crystal Growth, 2010, 312 (10): 1709–1716.
[67]. Geisler T. et al., J. of Non–Cryst. Solids, 2010, 356 (28): 1458–1465.
[68]. Matsusaka S. et al., Scripta Materialia, 2010, 62 (3): 141–143.
[69]. Ghosh S. et al., Int. J. of Hydrogen Energy, 2010, 35 (1): 272–283.
[70]. Bergeron B. et al., 12th Int. Conference on the Physics of Non–Cryst. Solids (PNCS 12), J. of Non–Cryst. Solids, 2010, 356 (44): 2315–2322.
[71]. Bonfils J. et al., J. of Non–Cryst. Solids, 2010, 356 (6): 388–393.
[72]. Dastjerdi M. H. T. et al., Electronics Letters, 2010, 46 (14): 1013–1014.
[73]. Yang G. et al., J. of the Euro. Ceram. Soc., 2010, 30 (4): 831–838.
[74]. Vayalakkara P. et. al., 2011, 37th IEEE: 003080–003083.
[75]. Dusserre G. et al., France, Europe: HAL CCSD, Elsevier, 2011.

[76]. Reibstein S. et al., J. of Chem. Phys., 2011, 134 (20): 204502.
[77]. Hrudananda J., J. of Non–Cryst. Solids, 2011, 357 (15): 2911–2919.
[78]. Bibler N., 2011, DOI: 10.2172/1001774.
[79]. Rose P. B. et al., J. of Non–Cryst. Solids, 2011, 357 (15): 2989–3001.
[80]. Zhang X. H. et al., Int. J. of Refractory Metals and Hard Materials, 2011, 29 (4): 495–498.
[81]. Villalpando–Reyna A. et al., Ceram. Int., 2011, 37 (5): 1625–1629.
[82]. Laopaiboon R. et al., Annuals of Nuclear Energy, 2011, 38 (11): 2333–2337.
[83]. Toshihiko H. et al., Elsevier, 2011, DOI: 10.1016/j.proeng.2011.04.123.
[84]. Kim C. E. et al., J. of Non–Cryst. Solids, 2011, 357 (15): 2863–2867.
[85]. Dharmadhikari J. A. et al., Optics Comm., 2011, 284 (2): 630–634.
[86]. Huang Z. et al., Thin Solid Films, 2011, 519 (13): 4246–4248.
[87]. Chhillar S., J. Radioanal Nucl. Chem., 2012, 294: 115–119.
[88]. Bootjomchai C. et al., Radiation Effects & Defects in Solids, 2012, 167 (4): 247–255.
[89]. Antropova T. V. et al., Physics of the Solid State, 2012, 54 (10): 2106–2111.
[90]. Hamodi N. H. et al., Int. J. of Appl. Glass Sci., 2012, 3 (3): 254–262.
[91]. Hamodi N. et al., New J. of Glass and Ceramics, 2012, 2: 111–120.
[92]. Du J. et al., Radiation Effects & Defects in Solids, 2012, 167 (1): 37–48.
[93]. Hao H. et al., 2012, DOI: 10.1109/ISAF.2012.6297806.
[94]. Levitskii A. et al., Glass and Ceramics, 2013, 70 (5): 6.
[95]. Eremyashev V. A. et al., Glass and Ceramics, 2013, 69 (9–10).
[96]. Zapol P. et al., Int. J. of Appl. Glass Sci., 2013, 4 (4): 395–407.
[97]. Ahamed M. J. et al., 2013, DOI: 10.1109/ICSENS.2013.6688574.
[98]. Yang K. J. et al., The 18th Int. Conference on Ion Beam Modifications of Materials (IBMM2012), Nuclear Inst. and Methods in Physics Research B, 2013, 307: 541–544.
[99]. Sengupta P. et al., J. Am. Ceram. Soc., 2015, 98 (1): 88–96.
[100]. Lai Y. et al., Int. Conference on Manipulation, Manufacturing and Measurement on the Nanoscale (3M–NANO) Manipulation, Manufacturing and Measurement on the Nanoscale (3M–NANO), 2015 International Conference, 2015.
[101]. Gautam C. et al., Spectroscopy Letters, 2015, 48: 280–285.
[102]. Cimek J. et al., Opt. and Quantum Electronics, 2015, 47 (1): 27–35.
[103]. Cheewasukhanont W. et al., 2015, DOI: 10.1109/ICICI-BME.2015.7401371.
[104]. Naberezhnov A. et al., Metal Science and Heat Treatment, 2015, 56 (11–12).
[105]. Mackel H. et al., J. Photovoltaics, IEEE Journal, 2015, 5 (4):1034–1046.
[106]. Kilymis D. A. et al., J. of Chem. Phys., 2015, 143 (9): 1–10.
[107]. Barlet M. et al., J. of Non–Cryst. Solids, 2015, 417–418: 66–79.
[108]. Jolley K. et al., 2015, DOI: 10.1016/j.nimb.2014.12.024.
[109]. Thorat V. S. et al., J. Am. Ceram. Soc., 2016, 99 (10): 3251–3259.
[110]. Weiwei H. et al., Elsevier, 2016, DOI: 10.1016/j.nimb.2016.05.016.
[111]. Sinev L. S. et al., Glass and Ceramics, 2016, 73 (1–2).
[112]. Boffy R. et al., J. of Neutron Research, 2016, 18: 97–107.
[113]. Wu L. et al., J. Am. Ceram. Soc., 2016, 99 (12): 4093–4099.
[114]. Dhara A. et al., J. of Non–Cryst. Solids, 2016, 1 (447): 283–289.
[115]. Wang T. S. et al., Surface & Coatings Techn., 2016, 306 Part A: 245–250.
[116]. Bouty O. et al., J. Mater. Sci., 2016, 51: 7918–7928.
[117]. Mylvaganam K. et. al., http://aepa2016.hiroshima-u.ac.jp/Home/Home.html (Access Date: 12.07.19).
[118]. Rathnaraj J. D. et al., 2017, DOI: 10.1109/ICRAAE.2017.8297228.
[119]. Shih Y. T. et al., 2017, DOI: 10.1111/jace.15059.

[120]. Ham K. J. et al., High Pressure Research, 2017, 37 (2): 233–243.
[121]. Ren M. et al., 2017, DOI: 10.1111/jace.14654.
[122]. Harris W. H. et al., J. of Amer. Ceram. Soc., 2017, DOI: 10.1111/jace.14895.
[123]. Pawar P. et al., 5th Int. Conference of Materials Processing and Characterization (ICMPC 2016), Materials Today: Proceedings 2017, 4 (2) Part A: 2813–2821, 2017.
[124]. Talimian A. et al., Int. J. of Appl. Glass Sci., 2017.
[125]. Del Cerro P. R. et al., 20th Int. Conference on Transparent Optical Networks (ICTON) Transparent Optical Networks (ICTON), 2018.
[126]. Meier S. et al., IEEE Journal, 2018, 8 (4): 982–989.
[127]. Ojansivu M. et al., PLoS ONE, 2018, 13 (8): e0202740.
[128]. Yuan W. et al., 2018, DOI: 10.1111/ijag.12348.
[129]. Mihailetchi V. D. et al., IEEE J. Photovoltaics, 2018, 8 (2): 435–440.
[130]. Soliman H. A. et al., 2018, DOI: 10.1111/ijag.12347.
[131]. Jinlong L. et al., Int. J. Adv. Manuf. Technol., 2018, 96: 1563–1569.
[132]. Ham K. J. et al., Materials, 2018, 1996–1944.
[133]. Schuhladen K. et al., J. of Non–Cryst. Solids, 2018, 502: 22–34
[134]. Nandi S. K. et al., 2016, DOI: 10.5772/63266.
[135]. Patel K. B., 10.17863/CAM.22955 (Access Date: 12.07.2019).
[136]. Ham K. J. et al., Materials, 2018, 11 (1): 114.
[137]. Lee J. C. et al., J. of Cleaner Production, 2019, 210: 638–645.
[138]. Wang M. et al., J. of Chem. Phys., 2019, 150 (4): 3.
[139]. Eremyashev V. E. et al., J. of Thermal Analysis and Calorimetry: An International Forum for Thermal Studies, 2019, 1–7.
[140]. Abdel–Hameed S. A. M. et al., Silicon, 2019, 11 (3): 1185–1192.
[141]. Alonso–Garcia M. C. et al., J. Photovoltaics, 2019, 9 (1): 331–338.
[142]. Guan M. et al., J. of Non–Cryst. Solids, 2019, 518:118–122.
[143]. Lv P. et al., J. of Nuclear Mater., 2019, 520: 218–225.
[144]. Wu L. et. al., J. of Nuclear Mater., 2019, 516: 152–159.
[145]. Du X. et al., Nuclear Sci. and Techn., 2019, 30 (7).
[146]. Prakash A. D. et al., J. of Non–Cryst. Solids, 2019, 510: 172–178.
[147]. Roldán Del Cerro P. et al., DOI: 10.1109/ICTON.2018.8473916.
[148]. Shaaban Kh. S. et al., 2019, 11: 4, 1853–1861.
[149]. Morsi R. M. M. et al., Silicon, 2019, 11: 1845.
[150]. Yuan W. et al., Int. J. of Appl. Glass Sci., 2019.
[151]. Weigel C. et al., 2019, DOI: 10.1109/TRANSDUCERS, 8808269.
[152]. Guan M., et al., J. of Non–Cryst. Sol., 2019, 518: 118–122.
[153]. Abdel–Hameed S. A. M. et al., Silicon, 2019, 11: 1185.
[154]. Lv P. et al., Elsevier, J. of Nuclear Mater., 2019, 520: 218–225.
[155]. Zhu H. et al., J. of Non–Cryst. Solids, 2019, 518: 57–65.
[156]. Karasu et al., El–Cezerî J. of Sci. and Eng., 2019, 6 (2): 299–322 (in Turkish).